

Skeletal Cut Loci on Convex Polyhedra

Joseph O’Rourke Costin Vilcu

March 1, 2024

Abstract

On a convex polyhedron P , the *cut locus* $\mathcal{C}(x)$ with respect to a point x is a tree of geodesic segments (shortest paths) on P that includes every vertex. We say that P has a *skeletal cut locus* if there is some $x \in P$ such that $\mathcal{C}(x) \subset \text{Sk}(P)$, where $\text{Sk}(P)$ is the 1-*skeleton* of P . At a first glance, there seems to be very little relation between the cut locus and the 1-skeleton, as the first one is an intrinsic geometry notion, and the second one specifies the combinatorics of P .

In this paper we study skeletal cut loci, obtaining four main results. First, given any combinatorial tree T without degree-2 nodes, there exists a convex polyhedron P and a point x in P with a cut locus that lies in $\text{Sk}(P)$, and whose combinatorics match T . Second, any (non-degenerate) polyhedron P has at most a finite number of points x for which $\mathcal{C}(x) \subset \text{Sk}(P)$. Third, we show that almost all polyhedra have no skeletal cut locus. Fourth, we provide a combinatorial restriction to the existence of skeletal cut loci.

Because the source unfolding of P with respect to x is always a non-overlapping net for P , and because the boundary of the source unfolding is the (unfolded) cut locus, source unfoldings of polyhedra with skeletal cut loci are edge-unfoldings, and moreover “blooming,” avoiding self-intersection during an unfolding process.

1 Introduction

Our focus is the cut locus $\mathcal{C}(x)$ on a convex polyhedron, and the relationship of $\mathcal{C}(x)$ to the 1-*skeleton* of P —the graph of vertices and edges—which we denote by $\text{Sk}(P)$. The *cut locus* $\mathcal{C}(x)$ of $x \in P$ is the closure of the set of points on P to which there is more than one geodesic segment (shortest path) from x . $\mathcal{C}(x)$ is a tree whose leaves are vertices of P . Nodes of degree $k \geq 3$ are *ramification points* to which there are k distinct geodesic segments from x . Nodes v of degree 2 in $\mathcal{C}(x)$ can also occur, if v is a vertex of P . For details, see Section 2.1.

The 1-skeleton of a non-degenerate polyhedron is a 3-connected graph by Steinitz’s theorem. We call a doubly-covered convex polygon a *degenerate* convex polyhedron, for which the 1-skeleton is a cycle. We say that P has a *skeletal cut locus* if there is some $x \in P$ such that $\mathcal{C}(x) \subset \text{Sk}(P)$.

The edges of $\mathcal{C}(x)$ are known to be geodesic segments [AAOS97], so it is at least conceivable that an edge of $\mathcal{C}(x)$ lies along an edge of P . Theorem 1 shows that, for certain polyhedra P and points $x \in P$, all of $\mathcal{C}(x)$ lies in the 1-skeleton of P : $\mathcal{C}(x) \subset \text{Sk}(P)$. As a simple example, we will see in Lemma 3 that the three edges incident to any vertex of a tetrahedron form $\mathcal{C}(x)$ for an appropriate x , and are therefore a skeletal cut locus.

Although Theorems 2 and 3 will show that skeletal cut loci are “rare” in senses we’ll make precise, Theorem 1 and its proof establish that uncountably many polyhedra do admit skeletal cut loci, in a sense made quantitatively precise by Proposition 1.

Theorem 4 characterizes those polyhedra every vertex of which has a skeletal cut locus. Complementing its first part, Theorem 5 provides a simple combinatorial restriction to the existence of skeletal cut loci, connecting to a current topic in graph theory.

Theorem 1 can also be viewed as a companion to the main result in [OV23], that any *length tree*—a tree with specified edge lengths—can be realized as the cut locus on some polyhedron. Here we only match the combinatorics of T , not its metrical properties, but requiring additionally for T to be included in $\text{Sk}(P)$.

Connection to Unfolding. It has long been known that cutting the cut locus $\mathcal{C}(x)$ and unfolding to the plane leads to the non-overlapping *source unfolding*: If x is not itself at a vertex, then the unfolding arrays all the shortest paths 2π around x , with the image of the cut locus forming the boundary of the unfolding [Mou85] [SS86]. For the polyhedra in Theorem 1, the source unfolding is an edge-unfolding. And because it is known that the source unfolding can be *bloomed*—unfolded continuously from \mathbb{R}^3 to \mathbb{R}^2 without self-intersection [DDH⁺11]—Theorem 1 and its companion Proposition 1 provide perhaps the first infinite class of examples of blooming edge-unfoldings.

A central open problem asks for an accounting of all the polyhedra P that support a skeletal cut locus. All of these enjoy the property that source unfoldings are also blooming edge-unfoldings.

2 Construction of Skeletal Cut Loci

Our first result is the following theorem.

Theorem 1 *Given any combinatorial tree T without degree-2 nodes there is a convex polyhedron P and a point $x \in P$ such that the cut locus $\mathcal{C}(x)$ is entirely contained in $\text{Sk}(P)$, and the combinatorics of $\mathcal{C}(x)$ match T .*

We first illustrate the main idea of the construction before addressing details. Suppose the given tree T is the 7-leaf tree shown in Fig. 1. We select a degree-3 node as root a , which corresponds to the apex of a regular tetrahedron $av_1v_2v_3$. We fix x at the centroid of the base Q .

Fig. 2(a) show one possible construction of P . The edges incident to a are clearly in $\mathcal{C}(x)$ with x at the centroid of the base triangle. All three base vertices

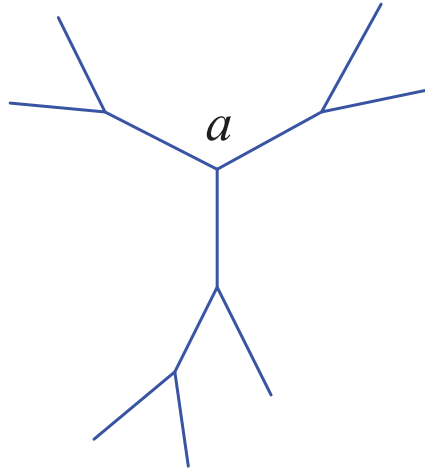


Figure 1: Tree T with 7 leaves.

of the tetrahedron are then truncated, with the truncation of v_1 truncated a second time. Now T corresponds to all the non-base edges of P .

The truncations are not arbitrary: the truncation planes must have precise tilts in order for the edges of each truncation to lie in $\mathcal{C}(x)$. Fig. 2(b) shows the source unfolding of P , with a_1, a_2, a_3 the three images of a . The red bisector rays from x through the truncation vertices on the base Q suggest that indeed any point p on a truncation edge is equidistant from x and therefore on $\mathcal{C}(x)$.

Returning to the need for precise tilts of the truncation planes, let z be the point on the edge av_1 through which the truncation plane passes, creating a truncation triangle zt_1t_2 . As indicated in Fig. 3, the tilt is uniquely determined by the location of z : the placement of z determines t_1, t_2 , and the edge t_1t_2 determines z .

2.1 Cut Locus Preliminaries

For the readers convenience, we list next several basic properties of cut loci, sometimes used implicitly in the following.

- (i) $\mathcal{C}(x)$ is a tree drawn on the surface of P . Its leaves are vertices of P , and all vertices of P , excepting x (if it is a vertex) are included in $\mathcal{C}(x)$. All points interior to $\mathcal{C}(x)$ of degree 3 or more are known as *ramification points* of $\mathcal{C}(x)$. All vertices of P interior to $\mathcal{C}(x)$ are also considered as ramification points, of degree at least 2; see e.g. Fig. 8.
- (ii) Each point y in $\mathcal{C}(x)$ is joined to x by as many geodesic segments as the number of connected components of $\mathcal{C}(x) \setminus y$. For ramification points in $\mathcal{C}(x)$, this is precisely their degree in the tree.

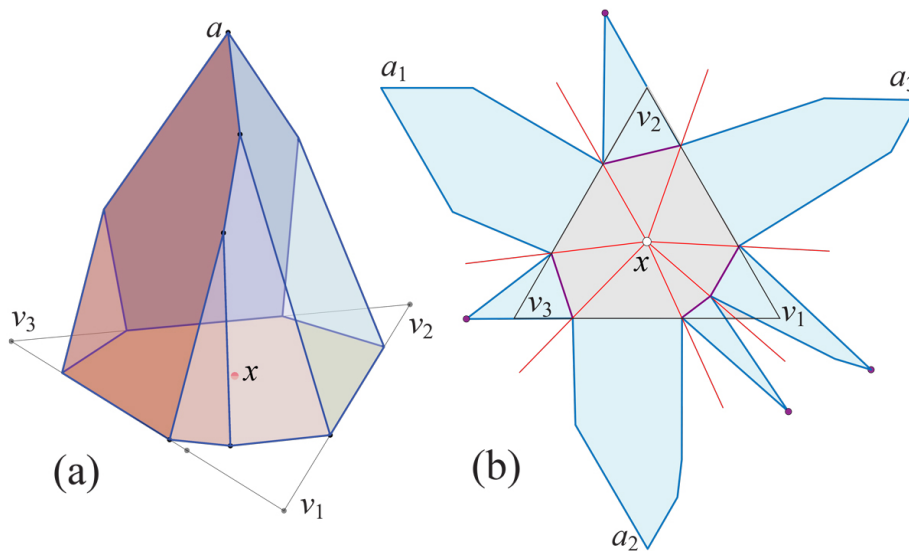


Figure 2: (a) P is created from a regular tetrahedron by four vertex truncations. $\mathcal{C}(x)$ consists of all non-base edges, and is homeomorphic to the tree in Fig. 1. (b) Source unfolding of P from x . Bisectors shown red.

- (iii) The edges of $\mathcal{C}(x)$ are geodesic segments on P .
- (iv) Assume the distinct geodesic segments γ and γ' from x to $y \in \mathcal{C}(x)$ bound a domain D of P , which intersects no other geodesic segment from x to y . Then there is an arc of $\mathcal{C}(x)$ at y which intersects D and bisects the angle of D at y .
- (v) The tree $\mathcal{C}(x)$ is reduced to a path, if and only if the polyhedron is a doubly-covered (planar) convex polygon, with x on the rim.

Further details and references can be found in [OV24, Ch. 2].

2.2 Construction Details

Throughout we assume T has no degree-2 nodes. Start with P a pyramid with apex a centered over a regular n -gon base Q , with x the centroid of Q . Label the vertices of Q as v_1, \dots, v_n .

The construction does not depend on the degree of apex a , so it is no loss of generality to assume a has degree-3 so that P starts as a regular tetrahedron. Let z be a node of T adjacent to a . (We will often use a and z and other variables to both refer to a node of T and a corresponding vertex of P .) Let z have degree $k + 2$ in T . Truncation of k planes through z will create a vertex at z of degree $k + 2$. E.g., if z is degree-3, $k = 1$ plane through z creates a vertex of degree-3, as we've seen in Fig. 3.

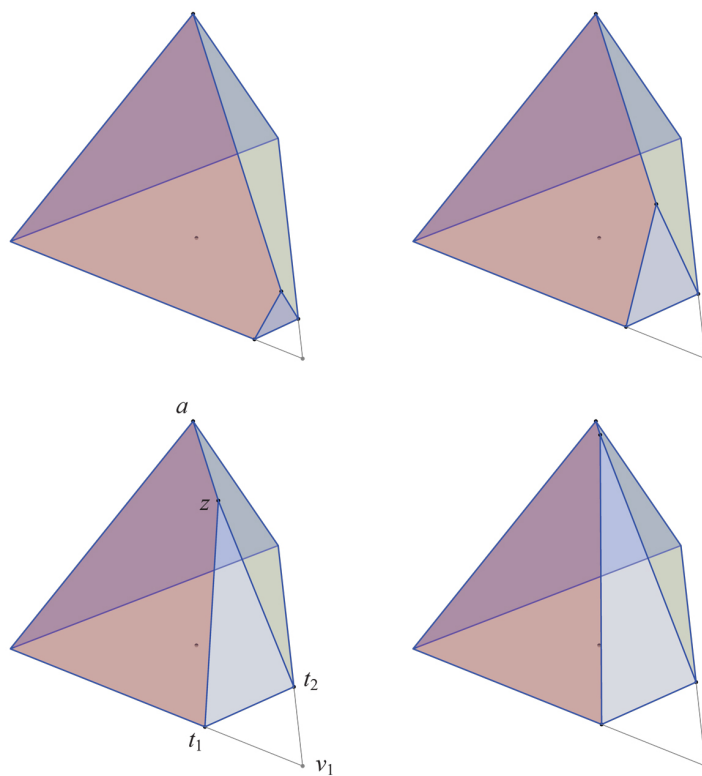


Figure 3: The tilt of the truncation plane is determined by the position of z on av_1 .

We aim to understand how to truncate $k \geq 1$ planes through z so that the $k+1$ truncation edges incident to the base Q are part of $\mathcal{C}(x)$. We will illustrate in detail the case $k = 2$ shown in Fig. 4. Looking ahead, if we know how to construct k planes through z , then we can apply the same logic to construct j planes through a child y of z . The $j = 1$ case is illustrated in Fig. 5, with the red truncation triangle incident to y . Then the same construction technique can be used to inductively create the full subtree rooted at z . We will show later that the subtrees rooted at the other two children of a can be arranged to avoid interfering with one another.

We express the construction as a multi-step algorithm, and later prove that the truncation edges are in $\mathcal{C}(x)$. Fix $k \geq 1$, and position z anywhere in the interior of av_1 . The goal is to compute the *truncation chain* $t_1, t_2, \dots, t_k, t_{k+1}$ on base Q , where $t_1 \in v_1v_n$ and $t_{k+1} \in v_1v_2$ (e.g., t_1, t_2, t_3 in Fig. 4). Each truncation triangle is then zt_it_{i+1} .

The construction of the truncation chain is effected by first computing the unfolded positions z_i , the images of z in the unfolding. It is perhaps counterintuitive, but we can calculate z_i without knowing t_it_{i+1} ; instead we use z_i to calculate t_it_{i+1} . The next construction depends of our choice of several parameters; we'll see later that it provides a suitable polyhedron.

- (1) z_0 is the position of z unfolded with the left face of the tetrahedron, av_3v_1 . z_0 can be determined by $|v_1z| = |v_1z_0|$. Then z_{k+1} is the reflection of z_0 across xv_1 .
- (2) Set $r_z = |xz_0| = |xz_{k+1}|$.
- (3) All the z_i 's are chosen to lie on the circle C_z centered on x of radius r_z .
- (4) Let A be the angle z_0xz_{k+1} . Partition A into $k+1$ angles α . This is another choice, to maximize the symmetry of the construction.
- (5) The z_i 's lie on rays from x separated by α . Together with C_z , this determines the location of the z_i 's.
- (6) Set B_i to bisect the angle at x between the z_{i-1}, z_i rays, $i = 1, \dots, k+1$.
- (7) We determine t_1 and t_{k+1} using the first and last bisector: $t_1 = v_1v_n \cap B_1$, $t_{k+1} = v_1v_2 \cap B_{k+1}$. The intermediate chain vertices t_2, \dots, t_k are not yet determined.
- (8) Let Π_i be the mediator plane through zz_i , the plane orthogonal to zz_i through its midpoint. It is these planes that determine t_i , $i = 2, \dots, k$.
- (9) Π_i intersects the xy -plane in a line L_i containing t_it_{i+1} .
- (10) $t_i = L_i \cap B_i$.

First note that the mediator plane construction of t_it_{i+1} guarantees that z unfolds to z_i . Second, the angles between edges t_iz_{i-1} and t_iz_i are split by B_i by construction. So any point p on the interior of edge zt_i unfolds to two images in the plane equidistant from x .

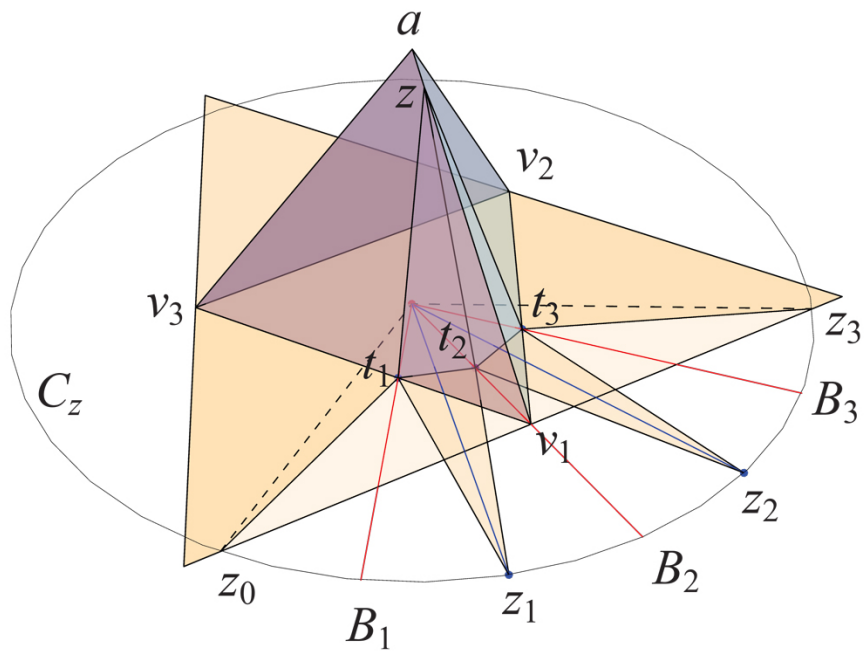


Figure 4: $k = 2$ truncation planes through z .

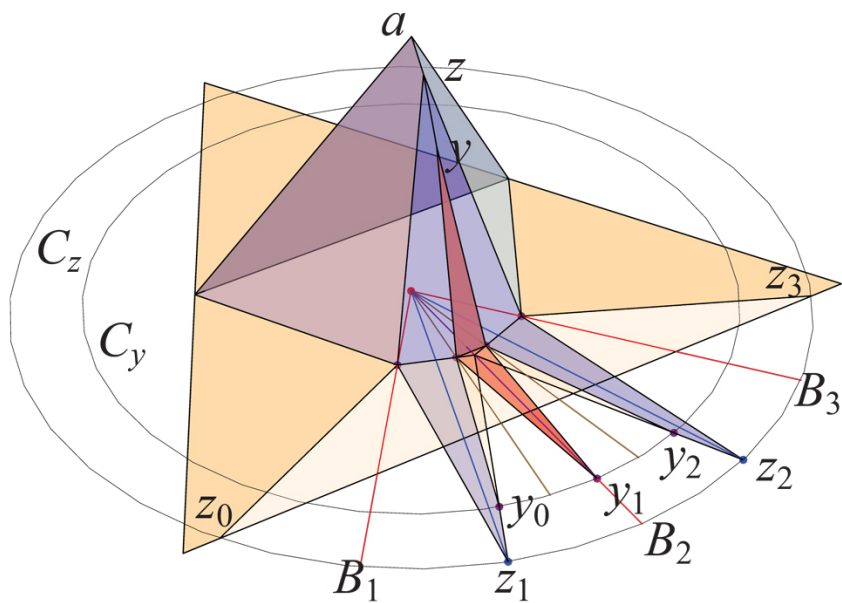


Figure 5: $k = 2, j = 1$. The y -truncation cuts the zt_2 edge in Fig. 4.

Lemma 1 *Each truncation edge zt_i is an edge of $\mathcal{C}(x)$.*

Proof: We first prove that zt_1 lies in $\mathcal{C}(x)$. Throughout refer to Fig. 6.

Before truncation, the segment zt_1 lies on the face av_3v_1 of the polyhedron P , which is a regular tetrahedron in this case.

Fix a point $p \in zt_1$. The unique shortest path γ to p crosses edge v_1v_3 . After truncation, γ remains a geodesic arc. We aim to prove that it remains shortest, and moreover there is another companion geodesic segment γ' , establishing that $p \in \mathcal{C}(x)$.

Now we consider the situation after truncation. Let δ be a geodesic arc from x to p , approaching p from the other side of zt_1 ; see Fig. 6(b). If δ crosses the edge t_1t_2 , then we have $|\gamma| = |\delta|$ by construction, and we have found $\gamma' = \delta$.

Suppose instead that δ crosses edge t_it_{i+1} for $i \geq 2$, and then crosses the truncation triangles $zt_it_{i+1}, zt_{i-1}t_i, \dots, zt_1t_2$ (right to left, i.e., clockwise, in Fig. 6(a)) before reaching p . To simplify the discussion, we illustrate $i = 2$, so δ crosses t_2t_3 and then triangles zt_2t_3 and zt_1t_2 . See Fig. 6(b).

Let q_2 be the quasigeodesic¹ xt_2z on P' ; it must be crossed by δ to reach p . There are two triangles xt_2z_1 and xt_2z_2 bounding q_2 to either side, congruent by the construction. Thus the construction has local intrinsic symmetry about q_2 .

Let s be the point at which δ crosses t_2t_3 , $\{s\} = \delta \cap t_2t_3$. First assume that s lies in the triangle xt_2z_2 . Then δ remains in xt_2z_2 until it crosses q_2 . Then there must be another geodesic arc δ' symmetric with δ about q_2 , as illustrated in (b). So δ and δ' meet at a point of q_2 . Because δ and δ' have the same length, neither can be a shortest path beyond that point of intersection. Therefore δ cannot reach p as a geodesic segment.

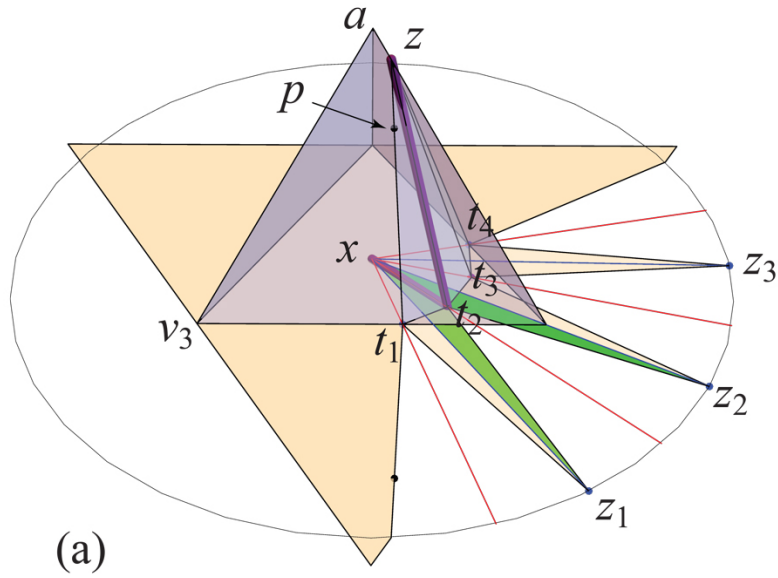
Second, if s instead lies in the triangle xt_3z_2 , then it is clear from the planar image in (a) of the figure that δ cannot cross the segment xz_2 clockwise, which it must to reach p from the right in the figures. So δ must head counterclockwise, crossing $q_3 = xt_3z$. Then the same argument applies, based this time on the local intrinsic symmetry about q_3 , and shows that δ cannot be a shortest path beyond q_3 .

We have established that every point p on zt_1 is on $\mathcal{C}(x)$, and so $zt_1 \subset \mathcal{C}(x)$. The same argument applies to zt_{k+1} , the rightmost truncation edge in the figures.

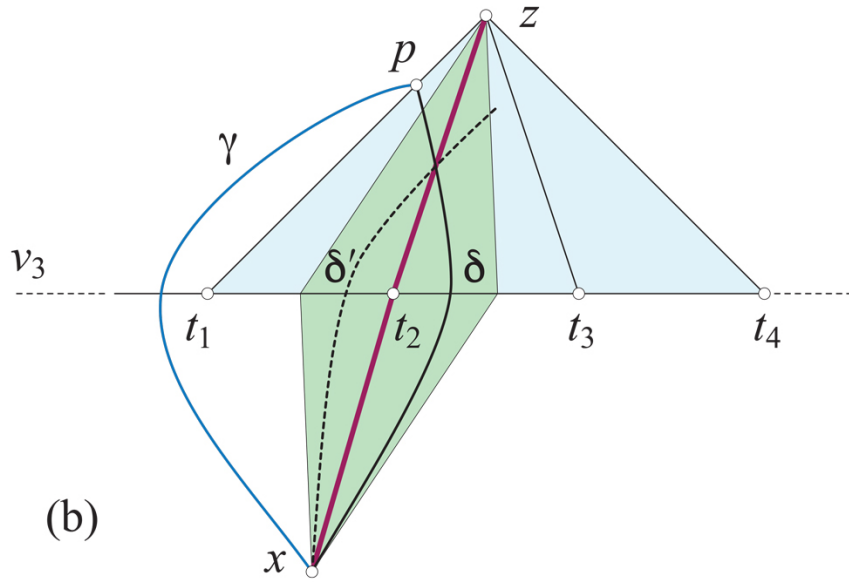
So now we know that two geodesic segments from x to z cross t_1t_2 and $t_k t_{k+1}$. These two segments determine a digon D within which the remaining segments of $\mathcal{C}(x)$ lie. But within D we have local intrinsic symmetry with respect to the quasigeodesics $q_i = xt_iz$, because q_i is surrounded by the congruent triangles xt_iz_{i-1} and xt_iz_i . Therefore, the previous argument shows that all the edges zt_i are included on $\mathcal{C}(x)$. \square

We now return to the claim that the three subtrees descendant from a do not interfere with one another.

¹A *quasigeodesic* is a path with at most π surface to either side of every point.



(a)



(b)

Figure 6: Proof that $p \in zt_1$ is on $\mathcal{C}(x)$. (a) Quasigeodesic $q_2 = xt_2z$ shown purple and congruent triangles xt_2z_1 and xt_2z_2 shaded green. (b) Abstract picture depicting geodesic segments γ, δ, δ' .

Lemma 2 *The truncations for one subtree descendant of apex a do not interfere with another subtree descendant.*

Proof: First, as $k \rightarrow \infty$, t_1 approaches the line xz_0 . This is evident in Fig. 11 where $k = 8$. Thus the leftmost truncation triangle stays to the v_1 -side of the midpoint of v_1v_3 , say by ε . Second, subsequent truncations to all but the extreme edges zt_1 and zt_{k+1} stay inside the t_1, \dots, t_k chain. The only concern would be that truncation of the zt_1 edge crossed the midpoint of v_1v_3 (and so possibly interfering with truncations of av_3). However, as is evident in the earlier Fig. 3, the position of t_1 moves monotonically toward v_1 as z moves down av_1 . Thus we can widen ε to accommodate a truncation of zt_1 (or of zt_{k+1}). So the entire subtree rooted at z stays between the midpoints of v_1v_3 and v_1v_2 . \square

Further examples are shown in Appendix A: $k = 4$ in Figs. 9 and 10, and $k = 8$ in Figs. 11 and 12.

Lemmas 1 and 2 together establish Theorem 1: $\mathcal{C}(x) \subset \text{Sk}(P)$ matches the given T .

3 Theorem 1 Discussion

We mentioned in Section 1 that Theorem 1 leads to an uncountable number of skeletal polyhedra. This follows immediately from the freedom to place z at any point interior to av_1 in the construction detailed in Section 2.2. We can be more quantitatively precise, as follows.

Assume that T is a cubic tree without degree-2 nodes, so it has n leaves and $n - 2$ ramification points. Aside from one ramification point, which is chosen as the apex of the starting tetrahedron, all others are free to vary on their respective edges in our construction, which implies $n - 3$ free parameters. Because $\mathcal{C}(x)$ is skeletal, each ramification point of T is a vertex of P , so P has $V = 2n - 2$ vertices, and $n = V/2 + 1$. The space \mathfrak{P}_V of all convex polyhedra with V vertices, up to isometries, has dimension $3V - 6$ (see for example [LP22]), hence the starting tetrahedron provides another 6 free parameters and we have the next result.

Proposition 1 *The set of convex polyhedra admitting skeletal cut loci—and hence blooming edge-unfoldings—contains a subset of dimension $\geq V/2 + 4$ in the $(3V - 6)$ -dimensional space of all convex polyhedra with V vertices, up to isometries.*

Recall we restricted Theorem 1 to trees T without degree-2 nodes. Our construction can be viewed as realizing degree-2 nodes of T with flat “vertices” on $\text{Sk}(P)$ —points interior to edges of P . We are currently extending the construction to match degree-2 nodes of T with non-flat vertices of P . See Fig. 7 for an example.

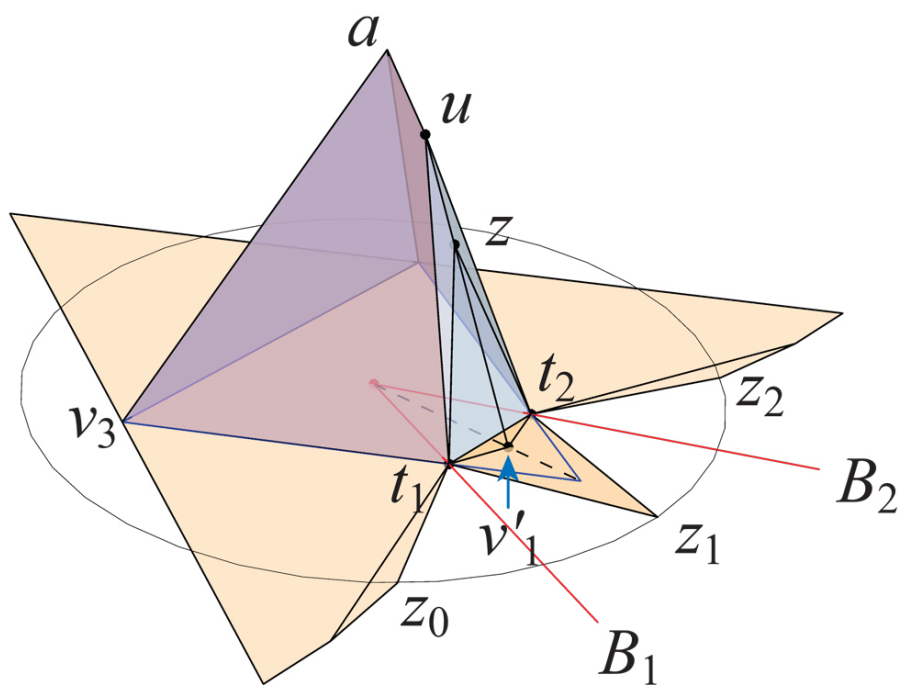


Figure 7: u is degree-2 node. $k = 1$ truncation at z . Edges ut_1 and ut_2 are not in $\mathcal{C}(x)$, but edges au , uz , and zt_1 and zt_2 , are in $\mathcal{C}(x)$.

Our construction for Theorem 1 results in a *dome*, a convex polyhedron P with a distinguished base face Q , with every other face sharing an edge with Q . It was already known that domes have edge-unfoldings [DO07, p. 325], although the proof of non-overlapping for our domes is almost trivial—the source unfolding does not overlap.

Although our previous construction results in domes, there are many other polyhedra with skeletal cut loci, see e.g. Fig. 8 and Theorem 4. Which leaves us with this central open problem: *Characterize all convex polyhedra P which admit skeletal cut loci.* The remainder of the paper addresses and partially answers this problem.

Several natural questions now suggest themselves:

- (1) For a fixed P , how many distinct points x can lead to skeletal cut loci? (Theorem 2).
- (2) Can all of $\text{Sk}(P)$ for a given P be covered by skeletal cut loci? (Proposition 2).
- (3) How common / rare are skeletal cut loci in the space of all convex polyhedra? (Theorem 3).
- (4) Are there restrictions for the existence of skeletal cut loci? (Proposition 2, Theorems 2 and 5).

4 Existence of Several Skeletal Cut Loci

In the first two questions in the list above, degenerate P play a special role:

Proposition 2

- (a) *There exists infinitely many points x with $\mathcal{C}(x) \subset \text{Sk}(P)$ if and only if P is degenerate.*
- (b) *There exists two points x_1, x_2 on P whose cut loci together cover $\text{Sk}(P)$ if and only if P is degenerate.*

Theorem 2 is then a corollary of claim (a). Before arguing for a quantitative statement of this theorem, we make two observations. First, for P degenerate, $\text{Sk}(P)$ is the rim of P , and for any x on the rim, $\mathcal{C}(x)$ is a subset of $\text{Sk}(P)$. So one direction (a) of the proposition is trivial. Second, a special case asks whether it could be that each vertex v of P leads to a skeletal cut locus $\mathcal{C}(v)$. The answer is YES, realized, for example, by the regular octahedron.

Theorem 2 *For any non-degenerate P with E edges, there are at most $2\binom{E}{2}$ flat points x of P such that $\mathcal{C}(x) \subset \text{Sk}(P)$.*

Proof: Assume there exists a flat point x of P , such that $\mathcal{C}(x) \subset \text{Sk}(P)$. Then x belongs to one or two faces, $x \in F_j$, with $j \in \{1, 2\}$. Let F denote either F_1 if $j = 1$, or the union $F_1 \cup F_2$ if $j = 2$.

Denote by v_i , $i \geq 3$, the vertices of F , and by e_i the edge of $\mathcal{C}(x) \subset \text{Sk}(P)$ incident to v_i and not included in F . Finally, denote by γ_i the geodesic segment from x to v_i .

Because $e_i \subset \mathcal{C}(x)$, γ_i and e_i together bisect the complete angle at v_i , by the bisection property (iv) of the cut locus. In other words, the straight extensions E_i into F by all e_i are concurrent: they intersect at the point x .

Now we count all the possible locations x over all edges of P . Consider a pair of edges e_i, e_j . Each has possible edge extensions from each endpoint. So the edge extensions are geodesic rays. Two such straight extensions could intersect several times on P . However, only their first intersection beyond the endpoints is a possible location for x . Each edge has two extensions, one from each endpoint, and because there are E straight extensions of the E edges of P , there are at most $2 \binom{E}{2}$ possible locations for x . \square

So this theorem settles the other direction of Proposition 2(a).

Now we prove Proposition 2(b), that only degenerate P allows covering $\text{Sk}(p)$ by only two cut loci.

Proof: If P is degenerate then any two points on its rim, but not on the same edge, satisfy the conclusion.

Assume now that P is non-degenerate and $x \in P$ such that $\mathcal{C}(x) \subset \text{Sk}(P)$. Then $\mathcal{C}(x)$ has at least one ramification point of degree $d \geq 3$, as it is known that only degenerate P support path cut loci. The d edges of $\mathcal{C}(x)$ lie in at least 3 faces of P . Then there exists a cycle in $\text{Sk}(P)$, formed by edges of those faces which are not in $\mathcal{C}(x)$. But such a cycle cannot be covered by only one other cut locus, which is a tree. \square

Example 1 Consider a regular dipyrmaid P over a convex $2m + 1$ -gon; see Fig. 8. One can see that, for every midpoint x of a “base edge” e , $\mathcal{C}(x)$ is included in $\text{Sk}(P)$. More precisely, $\mathcal{C}(x)$ contains all base edges other than e , and the two “lateral edges” opposite to x . In particular, this provides $2m + 1$ such points, for $V = 2m + 3$ vertices.

5 Absence of Skeletal Cut Loci

The following lemma will explain a condition in Theorem 3 to follow.

Lemma 3 Every tetrahedron T has four points $x \in T$ such that $\mathcal{C}(x) \subset \text{Sk}(T)$.

Proof: For each vertex v_i , denote by x_i the ramification point of $\mathcal{C}(v_i)$. It follows, from cut locus property (ii), that v_i is the ramification point of $\mathcal{C}(x_i)$. Then, by (i) and (iii), $\mathcal{C}(x_i)$ consists of the three edges incident to v_i . \square

The next theorem establishes the rarity of skeletal cut loci. In the statement, by *almost all* we mean “all in an open and dense set” in \mathfrak{P}_V .

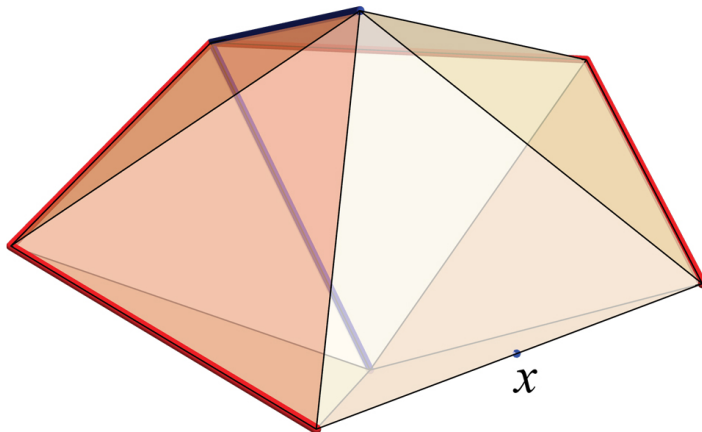


Figure 8: P : pentagonal dipyrmaid. $\mathcal{C}(x)$: red and blue edges of $\text{Sk}(P)$.

Theorem 3 *For almost all convex polyhedra P with $V > 4$ vertices, there exists no point $x \in P$ with $\mathcal{C}(x) \subset \text{Sk}(P)$.*

Note that Lemma 3 establishes the need for $V > 4$.

Proof: Notice first that almost all convex polyhedra P are non-degenerate.

Assume, for the simplicity of the exposition, that every face of P is a triangle and $\text{Sk}(P)$ is a cubic graph.

Case 1. Assume there exists a flat point x interior to some face F of P , such that $\mathcal{C}(x) \subset \text{Sk}(P)$.

Repeating the notation in Theorem 2, denote by v_i , $i = 1, 2, 3$, the vertices of F , and by e_i the edges of P incident to v_i and not included in F . Moreover, denote by γ_i the geodesic segment from x to v_i .

As in Theorem 2, it follows that $e_i \subset \mathcal{C}(x)$ so, together, γ_i and e_i bisect the complete angle at v_i . In other words, the straight extensions E_i into F by all the e_i are concurrent: they all intersect at the same point.

Now we perturb the vertices of P to destroy this concurrence. If P were a tetrahedron, then perturbing the apex would simultaneously move the edges incident to it. But the assumption that $V > 4$ means that there are at least two vertices outside the 3-vertex face F containing x . Perturbing these two vertices independently moves the edges incident to F independently, breaking the concurrence at x .

Because there are at most finitely many such points x by Theorem 2, the conclusion follows in this case.

Case 2. Assume there exists a flat point x interior to some edge e of P , such that $\mathcal{C}(x) \subset \text{Sk}(P)$. Denote by v_i , $i = 1, 2$, the vertices of e , and by e_i

the edges of P incident to v_i included in $\mathcal{C}(x)$. As above, it follows that the straight extensions of e_1, e_2 coincide with e . Now, small perturbations of the vertices of P destroy this coincidence. Note that if e, e_1, e_2 form a triangle, then e_1, e_2 will move together. But still, perturbations at other vertices of P (not $v_1, v_2, e_1 \cap e_2$) will destroy the concurrence.

Case 3. Assume finally there exists a vertex v of P , such that $\mathcal{C}(v) \subset \text{Sk}(P)$. Here we obtain again that the straight extensions of two edges contain (other) edge-pair extensions, and small perturbations of the vertices of P destroy this coincidence.

□

We mentioned that the octahedron has the property that for every vertex v , $\mathcal{C}(v)$ is skeletal. In the next section we detail the special conditions such polyhedra must satisfy.

6 Every Vertex a Skeletal Source

By Theorem 3, few convex polyhedra P have a point x with $\mathcal{C}(x) \subset \text{Sk}(P)$. So assuming that every vertex of P has this property should yield some exceptional polyhedra.

Theorem 4 *Assume that every vertex of P has a skeletal cut locus. Then the following statements hold.*

1. *Every face of P is a triangle.*
2. *Every vertex of P has even degree in $\text{Sk}(P)$.*
3. *The edges at every vertex v split the complete angle at v into evenly many sub-angles, every two opposite such angles being congruent.*
4. *If, moreover, every vertex of P has degree 4 in $\text{Sk}(P)$ then P is an octahedron:*
 - *with three planar symmetries, and*
 - *all faces of which are acute congruent (but not necessarily equilateral) triangles.*

Proof:

- (1) Assume there exists a non-triangular face F of P , so there are non-adjacent vertices u, v of F . Because $v \in \mathcal{C}(u) \subset \text{Sk}(P)$, there exists an edge vw of P with $vw \subset \mathcal{C}(u)$. Moreover, the diagonal uv of F and vw bisect the complete angle at v .

Because vw is an edge, it is a geodesic segment from w to v . So v is a leaf of $\mathcal{C}(w)$, and $\mathcal{C}(w)$ starts at v in the direction of the diagonal vu , hence $\mathcal{C}(w) \not\subset \text{Sk}(P)$.

- (2) Consider now a vertex u of P of degree d in $\text{Sk}(P)$, and denote by u_1, \dots, u_d its neighbors in $\text{Sk}(P)$.

For every u_i , $i = 1, \dots, d$, u is a leaf of $\mathcal{C}(u_i)$, so the edge $u_i u$ and the edge of $\mathcal{C}(u_i) \cap \text{Sk}(P)$ at u bisect the complete angle at u . Hence the edges at u can be paired two-by-two, hence their number is even.

- (3) Denote by $e_1, \dots, e_k, e_{k+1}, \dots, e_{2k}$ the edges sharing the vertex u , indexed circularly, and put $\alpha_i = \angle(e_i, e_{i+1})$, with index equality $2k + 1 = 1$.

The bisecting property of cut loci implies that the edge e_1 (as a geodesic segment from vertex u_1 to u) and the edge e_{k+1} (as the branch of $\mathcal{C}(u_1)$ at leaf u) bisect the complete angle at u :

$$\sum_{i=1}^k \alpha_i = \sum_{i=1}^k \alpha_{k+i}.$$

Similarly,

$$\sum_{i=2}^{k+1} \alpha_i = \sum_{i=2}^{k+1} \alpha_{k+i}.$$

Subtracting, we get $\alpha_1 = \alpha_{k+1}$.

Analogous reasoning implies the other equalities: $\alpha_i = \alpha_{k+i}$, with index equality $2k + j = j$.

- (4) For the combinatorial part, denote by F, E, V the number of faces, edges, and respectively vertices of P . Euler's formula for convex polyhedra gives $F - E + V = 2$. Our assumptions imply $3F = 2E$, and $4V = 2E$. These equations yield $V = 6$ and $F = 8$, hence P is an octahedron.

Denote by u, v, a, b, c, d the vertices of P , with a, b, c, d neighbor to both u and v .

Applying the hypothesis for a, b, c, d shows that the cycle $C = abcda$ in $\text{Sk}(P)$ is a bisecting polygon. Therefore, there exists a local isometry ι of the 'upper' and 'lower' neighborhoods N_u, N_v of C . In particular, the curvatures at u and v are equal, by Gauss-Bonnet.

It follows even more, that the local isometry ι extends to an intrinsic isometry between the 'upper' and the 'lower' closed half-surfaces bounded by C (regarding them as cones), hence it further extends to an isometry of P fixing C . Therefore, C is planar and P is symmetric with respect to the respective plane, by the rigidity part of Alexandrov's Gluing Theorem.

Repeating the reasoning for other pairs of 'opposite' vertices shows that all faces of P are congruent triangles.

The four faces sharing the vertex u have congruent angles at u , hence those angles are acute.

□

Example 2 *Suitable dipyramids over convex $2m$ -gons, similar to Example 1, provide non-octahedron polyhedra whose the cut loci of the vertices cover the 1-skeleton.*

7 A Combinatorial Restriction

Already mentioned in the Abstract, at a first glance there seems to be very little relation between the cut locus and the 1-skeleton, as the first one is an intrinsic geometry notion, and the second one specifies the combinatorics of P . A background connection between the two notions can however be established in two steps: Alexandrov’s Gluing Theorem connects the intrinsic and the extrinsic geometry of P , while Steinitz’s Theorem relates the combinatorics to the extrinsic geometry.

In this section we provide an easy combinatorial restriction to the existence of skeletal cut loci, complementing the first part of Theorem 4.

Lemma 2.8 in [OV24] shows that, at a vertex v of P of degree 3 in $\text{Sk}(P)$, the sum of any two face angles is strictly larger than the third angle. Therefore such a v cannot be a degree-2 node in a cut locus, because of Property (iv) of cut loci, proving the following.

Theorem 5 *A HIST-free cubic polyhedral graph cannot be realized with skeletal cut loci.*

A spanning tree without degree-2 nodes is called a *HIST* in the literature.²

One can check straightforwardly that, among the Platonic solids, the cube and the dodecahedron graphs are HIST-free, hence these polyhedra do not admit skeletal cut loci.

Acknowledgements. We thank Joseph Malkevitch for information on HISTs.

References

- [AAOS97] Pankaj K. Agarwal, Boris Aronov, Joseph O’Rourke, and Catherine A. Schevon. Star unfolding of a polytope with applications. *SIAM J. Comput.*, 26:1689–1713, 1997.
- [DDH⁺11] Erik D Demaine, Martin L Demaine, Vi Hart, John Iacono, Stefan Langerman, and Joseph O’Rourke. Continuous blooming of convex polyhedra. *Graphs and Combinatorics*, 27:363–376, 2011.

²HIST abbreviates “homeomorphically irreducible spanning tree.” See, e.g., [GNRZ24] and the references therein.

- [DO07] Erik D. Demaine and Joseph O’Rourke. *Geometric Folding Algorithms: Linkages, Origami, Polyhedra*. Cambridge University Press, 2007. <http://www.gfalop.org>.
- [GNRZ24] Jan Goedgebeur, Kenta Noguchi, Jarne Renders, and Carol T Zamfirescu. HIST-critical graphs and Malkevitch’s conjecture. arXiv:2401.04554., 2024.
- [LP22] Nina Lebedeva and Anton Petrunin. Alexandrov’s embedding theorem. arXiv:2212.10479, 2022.
- [Mou85] David M. Mount. On finding shortest paths on convex polyhedra. Technical Report 1495, Dept. Computer Science, Univ. Maryland, 1985.
- [OV23] Joseph O’Rourke and Costin Vilcu. Cut locus realizations on convex polyhedra. *Comput. Geom.: Theory & Appl.*, 114, 2023. doi.org/10.1016/j.comgeo.2023.102010.
- [OV24] Joseph O’Rourke and Costin Vilcu. *Reshaping Convex Polyhedra*. Springer-Verlag, 2024. ISBN 978-3-031-47510-8. In press.
- [SS86] Micha Sharir and Amir Schorr. On shortest paths in polyhedral spaces. *SIAM J. Computing*, 15(1):193–215, 1986.

A Appendix: Theorem 1 Examples

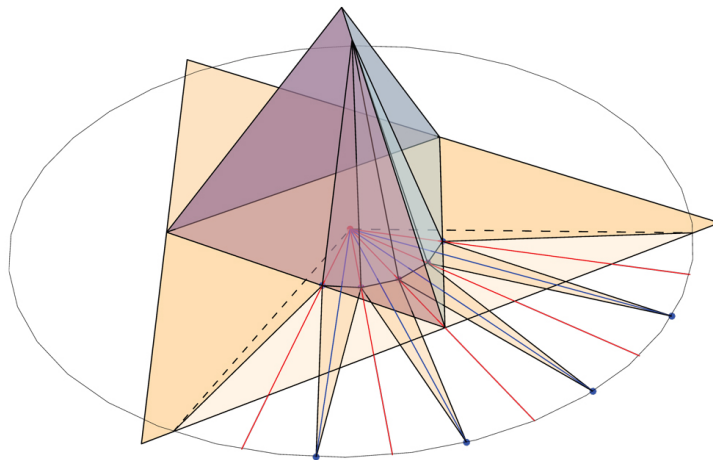


Figure 9: $k = 4$.

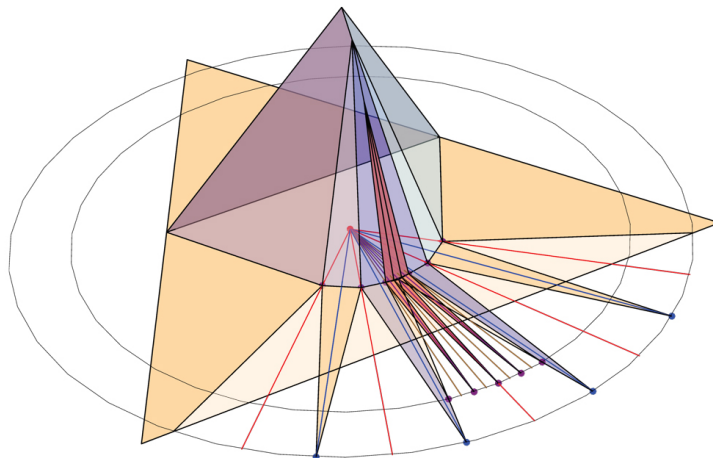


Figure 10: $k = 4, j = 3$.

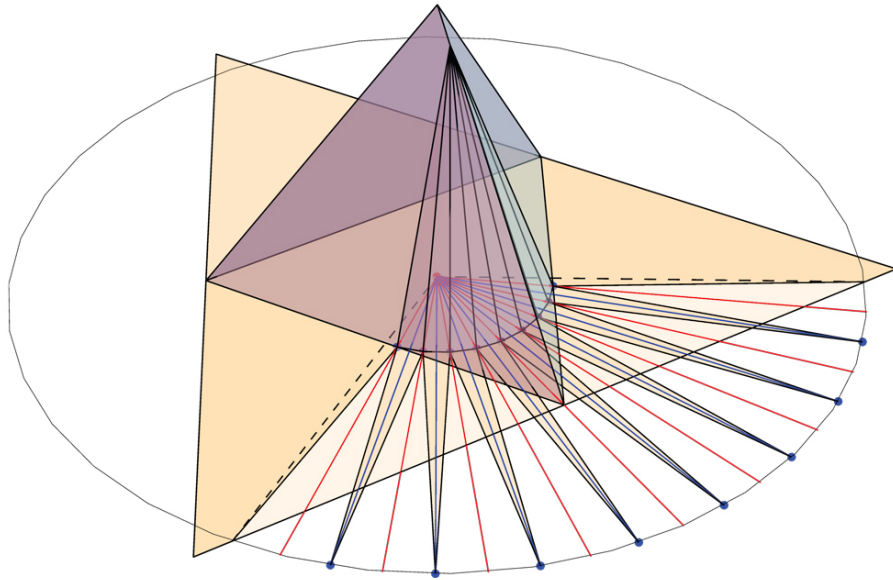


Figure 11: $k = 8$.

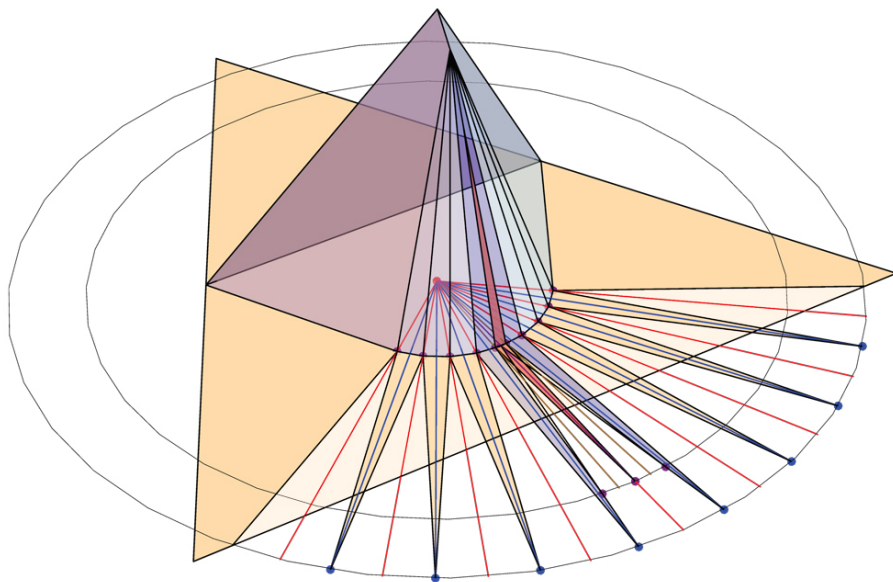


Figure 12: $k = 8, j = 1$.